Journal of Fluorescence, Vol. 7, No. 4, 1997

Dipole Moments of Phenylnaphthylamine Fluorescence Probes and Study of Dielectric Interactions in Human Erythrocyte Ghosts

N. A. Nemkovich,[1,3] W. Baumann,[2] Yu. V. Kruchenok,[1] H. Reis,[2] and A. N. Rubinov[1]

Received October 27, 1997; revised January 20, 1998; accepted January 23, 1998

Electrooptical absorption and emission methods were used to measure the dipole moments of 1-phenylnaphthylamine (1-AN) and 1,8-anilinonaphthalene sulfonate (1,8-ANS) fluorescence probes in the ground and excited states. The measurements were performed in cyclohexane (1-AN) and dioxane (1-AN and 1,8-ANS). Our results show that the charge distribution in 1-AN differs substantially from that in 1,8-ANS. The spectral dependence of electrooptical coefficients in the case of 1,8-ANS indicates that the absorption band is a superposition of several (at least two) electronic transitions. We found that the electronic spectra of 1-AN in erythrocyte ghosts are inhomogeneously broadened. Due to inhomogeneous broadening it is possible to excite selectively molecules located at different sites. Dielectric interactions (given by the dielectric constant) were investigated from the position of the maximum of the fluorescence quantum spectra of 1-AN. The dielectric constant of human erythrocyte ghosts varies from about 6.7 ± 0.8 to about 17.6 ± 3.5, depending on the excitation frequency and, consequently, on the location of the probe.

KEY WORDS: Absorption; fluorescence probe; dipole moment; electro-optical method; dielectric constant; erythrocyte ghosts.

INTRODUCTION

Phenylnaphthylamine fluorescence probes, especially 1-phenylnaphthylamine (1-AN) and 1,8-anilinonaphthalenesulfonate (1,8-ANS), have been widely used to obtain information about proteins, enzymes, membranes, and other biological systems.[1-7] These probes are interesting candidates not only from the view of applications, but also with respect to an understanding of absorption and emission mechanisms. The long-wavelength electronic transitions in aromatic hydrocarbons having strongly conjugating substituents, such as amines, have been interpreted as a combination of the local states of two parts of a "composite molecule" plus a certain percentage of electron-transfer states between the two components.[8]

The usefulness of 1-AN and 1,8-ANS probes follows from the marked sensitivity of their fluorescence characteristics to the properties of the environmental medium. For example, the quantum yields of 1-AN and its sulfonate derivative 1,8-ANS are enhanced essentially when they are transferred from a polar to a nonpolar medium, as first recognized by Weber and Laurence.[9] In addition, a substantial blue shift in the position of fluorescence spectrum takes place. A number of papers were published concerning the strong solvent dependence of 1-AN, 1,8-ANS, and related spectral properties.[1-4,10,11] It was concluded that the large wavelength shift of the fluorescence spectrum results from solvent relaxation during the exited-state lifetime caused by essential change of the probe dipole moment after excitation.

[1] B. I. Stepanov Institute of Physics, Academy of Sciences of Belarus, F. Skaryna Avenue 70, 220072 Minsk, Belarus.
[2] Institute of Physical Chemistry, University of Mainz, Jakob Welder-Weg 11, 55099 Mainz, Germany.
[3] To whom correspondence should be addressed. Fax: 375 17 239 3131. e-mail: nemkov@ifanbel.bas-net.by

1053-0509/97/1200-0363$12.50/0

Because of their properties, 1-AN, 1,8-ANS, and other fluorescence probes have found wide applications for the determination of micropolarity when bound to complex macromolecules, for example, to membranes.[10–16] Biological membranes are composed of proteins and lipid bilayers. The local dielectric interactions in membranes are the most important factor because electric forces between proteins or their segments are essential for their functions. On the other hand, intermolecular potentials are divided by a dielectric constant and due to this, for instance, a 10-fold change in the local dielectric constant can change the intermolecular potentials by as much as 10 times in magnitude. The lack of knowledge about the local dielectric constants of membranes has so far limited progress in understanding about interactions between proteins.

The best-known method for the determination of the local dielectric constant in complex macromolecules is based on using standard equations, describing the dependence of the position of the electronic spectra of the fluorescence probe on the dielectric constant, the refractive index, and the dipole moments of the probe in the ground and excited states. If the dipole moments in the relevant electronic states are known, the local dielectric constant may be determined by these equations from the position of the electronic spectra.

Electrooptical absorption and emission measurements in solution provide valuable information about the values and directions of the dipole moments in the ground and excited states of solute molecules.[17–19] Comparing electrooptical measurements with variants of solvent shift methods, the strong advantage of electrooptical measurements is that the dipole moments are determined in a single solvent, and hence it is possible to study the influence of the solvent on the process of intramolecular charge redistribution in the ground and excited electronic states. In addition, all solvent shift methods require an estimate of the probe cavity radius.

In this paper we describe the investigation by electrooptical absorption and emission methods of the equilibrated ground-state, excited Franck–Condon-state, and equilibrated excited-state dipole moments of 1-AN and 1,8-ANS in solutions. Additionally, we obtained the spectral inhomogeneity of 1-AN probe molecules in membranes and studied the local dielectric properties of human hemoglobin-free erythrocyte ghosts.

METHODS

The determination of ground- and excited-state dipole moments from electrooptical measurements has been presented fully in previous papers.[18,19] So only the basic principles of electrooptical absorption (EOAM) and integrated electrooptical emission (IEOEM) measurements in solution are briefly summarized here. Using Liptay's formalism,[17] the effect of an external electric field E_f on the molar absorption coefficient $\kappa(\tilde{\nu})$ can be described by a quantity L, which is defined by

$$L = L(\tilde{\nu}, \chi) = [\kappa^E(\tilde{\nu}, \chi) - \kappa(\tilde{\nu})]/\kappa(\tilde{\nu})E_f^2 \quad (1)$$

where κ^E is the molar absorption coefficient in the presence of an applied electric field, χ is the angle between the direction of E_f and the electric field vector of the incident light, and $\tilde{\nu}$ is the wavenumber. For a homogeneously broadened absorption band, L is given by[17–19]

$$L = Dr + [1/6]Es + Frt + Gst + Hru + Isu \quad (2)$$

where the parameters r and s are determined by the angle χ, and the quantities t and u depend on the first and second derivatives of the absorption spectrum,

$$r = (2 - \cos^2\chi)/5 \quad (3)$$

$$s = (3\cos^2\chi - 1)/5 \quad (4)$$

$$t = (1/hc)(\kappa/\tilde{\nu})^{-1} d(\kappa/\tilde{\nu})/d\tilde{\nu} \quad (5)$$

$$u = (\frac{1}{2} h^2c^2)(\kappa/\tilde{\nu})^{-1} d^2(\kappa/\tilde{\nu})/d\tilde{\nu}^2 \quad (6)$$

For the molecules discussed in this communication, explicit polarizability and transition polarizability effects can be neglected compared with the electric dipole moment terms. Then the coefficients D, E, F, G, H, and I are as follows:

$$D = 0 \quad (7)$$

$$E = (1/kT)^2 f_e^2 [3(\mathbf{m}_a\boldsymbol{\mu}_g) - \boldsymbol{\mu}_g^2] \quad (8)$$

$$F = (1/kT) f_e^2 (\boldsymbol{\mu}_g \boldsymbol{\Delta}^a\boldsymbol{\mu}) \quad (9)$$

$$G = (1/kT) f_e^2 (\mathbf{m}_a\boldsymbol{\mu}_g)(\mathbf{m}_a\boldsymbol{\Delta}^a\boldsymbol{\mu}) \quad (10)$$

$$H = f_e^2(\boldsymbol{\Delta}^a\boldsymbol{\mu})^2 \quad (11)$$

$$I = f_e^2(\mathbf{m}_a\boldsymbol{\Delta}^a\boldsymbol{\mu})^2 \quad (12)$$

where k is the Boltzmann constant, T is the temperature, $\mathbf{m}_a$ is the unit vector in the direction of the transition moment for absorption, $\boldsymbol{\mu}_g$ is the equilibrated ground-state dipole moment vector, and $\Delta^a\mu$ is the change of the dipole moment vector upon excitation to the considered Franck–Condon excited state. From a set of these five coefficients, the values of μ_g, $\Delta^a\mu$, and the angles between the transition moment $\mathbf{m}_a$ and $\boldsymbol{\mu}_g$ and $\boldsymbol{\Delta}^a\boldsymbol{\mu}$ can be determined. The cavity field correction f_e is defined according to Onsager's model as introduced to the elec-

trooptical methods by Liptay:[17]

$$f_e = 3\varepsilon/(2\varepsilon+1) \quad (13)$$

where ε is the relative permittivity of the solvent. The experimental setup for EOAM has been described in detail previously.[18,19] The quantity $L(\tilde{\nu}, \chi)$ in the present work was determined for two values of the angle $\chi(\chi = 0$ and $\chi = \pi/2)$ and for a set of wavenumbers within the first absorption band. Then the coefficients in Eqs. (7)–(12) and their standard deviations were obtained by multiple linear regression. For correct statistical weighting reasons the multiple linear regression was performed with the quantity $LK/\tilde{\nu}$, where K is the absorption coefficient.

The electric dipole moment μ_e in the equilibrated excited state has been determined by integral electrooptical emission measurements (IEOEM) as described in Ref. 20. The theory of IEOEM is given in Refs. 21 and 22 and the experimental setup for IEOEM is described in Ref. 18.

LASER SPECTROFLUORIMETER AND MATERIALS

Time-resolved fluorescence characteristics were measured by an automated laser spectrofluorimeter described in detail in Ref. 23. The excitation of this setup includes an atmospheric pressure nitrogen laser (pulse half-width, 0.35 ns; peak power, 350 kW) and a distributed-feedback dye laser (tuning range, 400–750 nm; spectral width, 0.1–0.6 nm). After passing the polarizer (Glan prism) the exciting radiation is directed on the sample, which is placed in front of an analyzing polarizer (Glan prism). The recording part of the apparatus includes a double diffraction monochromator (1200 lines/mm replica, 0.6 nm/mm dispersion). A FEU-164 photomultiplier (1.8-ns temporal resolution) records the optical radiation. The output signal of the photomultiplier is fed into a V4-24 boxcar integrator (1.0-GHz transmission band). The registered signal is normalized on the reference signal from the photodiode. The data are input into an IBM PC/AT-386. The laser spectrofluorimeter is fully automated; all optical and electronic systems are controlled by the computer. The coefficients for correction of the spectral sensitivity of the detection system were determined by a conventional method using a tungsten band lamp. The use of the deconvolution procedure allows improvement of the temporal resolution to ~50 ps for single-exponential fluorescence lifetime measurements and to ~200 ps for the registration of time-resolved spectra. The steady-state fluorescence spectra were registered by a spectrofluorimeter SFL-112A.

The deconvolution procedure is based on the modulating function method[24] combined with truncated singular value decomposition,[25] thus resembling the implementation by Striker,[26] though with slight differences. The fitting procedure is a nonlinear minimization reconvolution routine based on a combination of the Nelder–Mead simplex method[27] and the "switching method."[28]

Figure 1 presents the 1-AN and 1,8-ANS molecules studied in this work. The purity of 1-AN and 1,8-ANS was checked by thin-layer chromatography. The solvents (cyclohexane and dioxane) were purified by methods described in Ref. 29. The purified solvents were dried prior to use in the electrooptical measurements by distillation under reflux conditions over sodium/potassium alloy employing an argon atmosphere. The purity of the solvents was checked by UV absorption measurements (1-cm cell; reference, air).

To obtain the human red blood cell membranes we used fresh hemoglobin-free ghosts of human erythrocytes, prepared by a method originally described by Dodge *et al.*[30] All reagents and chemicals used were of the purest grade available from commercial sources. Human blood was provided by the Research Institute of Blood, Ministry of Public Health of Belarus.

ELECTROOPTICAL MEASUREMENTS

1-Phenylnaphthylamine Probe (1-AN)

We found that 1-AN shows coefficients E, F, and G practically equal to zero. This is not surprising because from the empirical calculations[31,32] and solvent shift measurements,[33] it is known that the dipole moment of 1-AN in the equilibrated ground state has a very small value μ_g, within $3.0–6.0 \times 10^{-30}$ Cm. As follow from our experiments in the case of 1-AN, only coefficients H and I can be measured with sufficient accuracy. In Table I the electrooptical coefficients obtained by multilinear regression analysis according to Eq. (2) with Eqs. (3)–(12) for 1-AN in cyclohexane and dioxane at $T = 298$ K are presented. As can be seen from Table I, the coefficients H and I are equal within the experimental error. This means that the vectors $\mathbf{m}_a$ and $\Delta^a\mu$ are parallel and an average value of $\Delta^a\mu$ can be determined from Eqs. (11) and (12).

In Table II, the values $\Delta^a\mu$ and μ_e calculated from the EOAM and IEOEM measurements for 1-AN are presented. The value of vector $\Delta^a\mu$ was found from the

1-Phenylnaphthylamine (1-AN) 1,8-Anilinonaphthalenesulfonate (1,8-ANS)

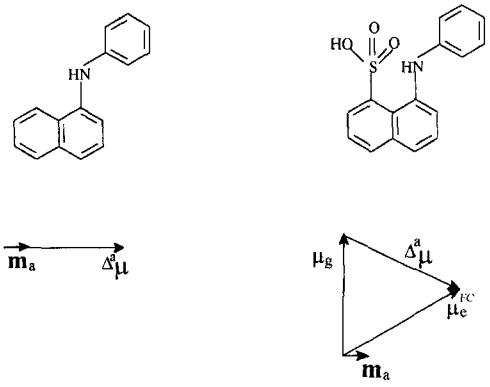

Fig. 1. Fluorescence probes studied in this work and diagrams of their different dipole moments. The orientations of transition dipole moments relative to the structural formulas are arbitrary.

Table I. Results of Electrooptical Absorption Measurements on 1-AN in Cyclohexane and Dioxane at T = 298 K (For Coefficients E, F, and G, See the Text)

Coefficient	Solvent, cyclohexane; spectral region of EOAM, 26,900–31,300 cm^{-1}	Solvent, dioxane; spectral region of EOAM, 26,300–31,300 cm^{-1}
H (10^{-60} C^2 m^2)	374 ± 19	510 ± 26
I (10^{-60} C^2 m^2)	368 ± 19	549 ± 26

Table II. Dipole Moments of 1-AN in Cyclohexane and Dioxane at T=298 K

Solvent	$\Delta^a\mu$ (10^{-30} Cm)	μ_e (10^{-30} Cm)
Cyclohexane	16.0 ± 1.0	16.4 ± 1.1
Dioxane	18.8 ± 0.9	24.6 ± 1.0

Table III. Electrooptical Coefficients Obtained by EOAM for 1,8-ANS in Dioxane at T=298 K

Coefficient	Spectral region of EOAM: 25,600–28,100 cm^{-1} (red slope)
E (10^{-20} V^{-2} m^2)	−3313 ± 15
F (10^{-40} CV^{-1} m^2)	−445 ± 24
G (10^{-40} CV^{-1} m^2)	−2 ± 24
H (10^{-60} C^2 m^2)	435 ± 78
I (10^{-60} C^2 m^2)	554 ± 78

formula

$$\Delta^a\mu = \frac{1}{f_c}\sqrt{\frac{H+I}{2}} \tag{14}$$

The values $\Delta^a\mu$ and μ_e determined for 1-AN in this work agree quite well with the solvent shift measurements performed by Kawski and Pasztor,[33] who obtained a dipole moment of 17.3 × 10^{-30} Cm for the first excited state, for the free molecule, and with the molecular orbital simulations performed in Refs. 31 and 32, which gave μ_e = 20.0 × 10^{-30} Cm.

1,8-Anilinonaphthalenesulfonate Probe (1,8-ANS)

In the case of 1,8-ANS in dioxane the situation is unlike that for 1-AN. The experimental electrooptical data are well approximated by the multilinear fit function in the spectral region 25,600–28,100 cm^{-1}, but coefficients E and F have negative values and coefficient G is roughly equal to zero (see Table III). The large negative value of E and very small value of G are real evidence that dipole moment $\mathbf{m}_a$ is perpendicular to vector $\boldsymbol{\mu}_g$ [see Eqs. (4) and (6)]. This conclusion agrees with molecular orbital calculations for 1,8-ANS made in Ref. 32. Assuming $\mathbf{m}_a \perp \boldsymbol{\mu}_g$ and assuming that all vectors lie in the naphthalene ring plane, the values of μ_g, $\Delta^a\mu$, and μ_e^{FC} and the angles between the different dipole moments can be evaluated from coefficients E, F, and I using Eqs. (8), (9), and (12). The results are shown in Table IV.

The origin of the strong solvent effect on the quantum yield of 1,8-ANS has been discussed extensively.[1-4,8-11] However, there seems to be no consensus and the strong solvent influence on the quantum yield has been attributed to different causes. Kosower *et al.*[34-37] have pointed out that there are two emitting excited singlet species: $S_{1,np}$, a species having a distinctly nonplanar structure whose fluorescence quantum yield is not sensitive to solvent; and $S_{1,ct}$, a charge-transfer species whose emission is solvent dependent. The initial nonplanar $S_{1,np}$ excited state is transformed into the charge-transfer state $S_{1,ct}$ Li *et al.*[38] argue that the large effect of polar solvents on the quantum yield may be due to a solvent-induced inversion of two excited states, ^1L_a and ^1L_b, of the α-isomer. Ebbesen and Ghiron[39] investigated the excited-state properties of 1,8-ANS in binary water–ethanol solutions. They concluded that the intramolecular charge-transfer and specific solvent–solute interactions are probably both involved in the case of 1,8-ANS.

Our results provide support for the existence of two close-lying excited Franck–Condon states of 1,8-ANS, at least in dioxane. We found that electrooptical coeffi-

Table IV. Dipole Moments and Angles Between the Different Moments of 1,8-ANS in Dioxane at $T=298$ K (Spectral Region of EOAM: 25,600–28,100 cm^{-1}; red slope)

μ_g (10^{-30} Cm)	$\Delta^a\mu$ (10^{-30} Cm)	μ_c^{FC} (10^{-30} Cm)	$\langle(\Delta^a\boldsymbol{\mu},\mathbf{m}_a)$	$\langle(\boldsymbol{\mu}_c^{FC},\mathbf{m}_a)$	$\langle(\boldsymbol{\mu}_c^{FC},\boldsymbol{\mu}_g)$	$\langle(\boldsymbol{\mu}_g,\Delta^a\boldsymbol{\mu})$
19.4 ± 0.1	20.3	23.3	18°	34°	56°	108°

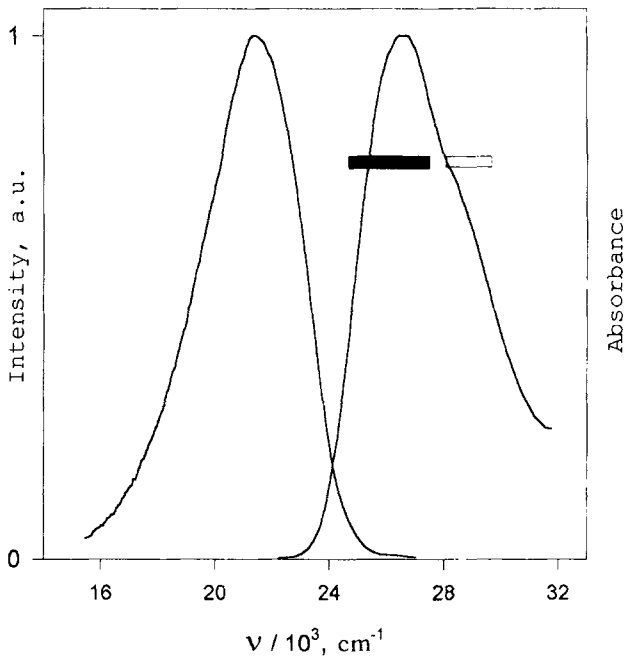

Fig. 2. Absorption and fluorescence spectra of 1,8-ANS in dioxane. The open and filled bars indicate the spectral range of EOAM at the long- and short-wavelength edges of the absorption spectrum.

cients F, G, H, and I determined at the short-wavelength edge of the absorption spectrum differ essentially from those obtained at the long-wavelength edge of the spectrum (see Fig. 2). Coefficient I in the spectral region 27,300–28,800 cm^{-1} (open bar in Fig. 2) has a negative value, which is theoretically impossible for a homogeneously broadened band. On the other hand, coefficients E measured in different spectral regions, and consequently, dipole moment μ_g [see Eq. (6)], are roughly the same. Because there is no essential overlap between the first and the second absorption band in the spectral region of EOAM 27,300–28,800 cm^{-1}, the results mentioned above are real evidence for the existence of two close-lying transitions inside the first absorption band. It seems likely that 1,8-ANS has two close-lying excited electronic states with different charge distributions and dipole moments.

Fluorescence lifetimes are very sensitive regarding various processes in the excited state. We measured the fluorescence lifetime τ_{fl} to check the homogeneity of the fluorescence band of 1,8-ANS in dioxane. The results show that the value of τ_{fl} measured at the blue and red edges of the fluorescence spectrum are equal within experimental error (13.1 ± 0.2 ns at ν_{reg} = 19,200 cm^{-1} and 13.2 ± 0.2 ns at ν_{reg} = 23,000 cm^{-1}). This fact supports that the fluorescence band is homogeneously broadened on the subnanosecond time scale. If the existence of different excited states is assumed, the independence of τ_{fl} on the detection wavelength may be explained by the low value of the quantum yield and the fast decay value one of the states on a time scale which is outside our time resolution.

SPECTRAL INHOMOGENEITY OF PROBE MOLECULES IN MODEL BIOLOGICAL MEMBRANES

As the incorporation of a probe into the membrane is a statistical process, a certain distribution of the probe over different locations (sites) may take place. Therefore different electrical fields may be applied to the probe at different sites. This results in statistical variation of the energy of intermolecular interactions of the probe with the environment and, consequently, in inhomogeneous broadening of its (probe) electronic spectra.

The effect of spectral inhomogeneity manifests itself in the shift of the fluorescence spectrum toward longer wavelengths under the shift of the excitation frequency to the red edge of the absorption band. In recent years red-edge excitation spectroscopy has become widely accepted as a general spectroscopic method for investigation not only of solutions,[40] but also of a number of biological systems.[6] In our previous papers[15,16,40-43] we have studied the spectral inhomogeneity of 1-AN probe in solutions and phospholipid bilayer membranes (vesicles) using stationary and time-resolved methods. The results obtained in the present paper prove the existence of spectral inhomogeneity for 1-AN probe mol-

ecules also in hemoglobin-free ghosts of human erythrocytes.

Experimentally obtained dependencies of the fluorescence spectrum maximum on the excitation frequency for 1-AN in erythrocyte ghosts prepared from two probes of blood are shown in Fig. 3. The difference between curve 1 and curve 2 demonstrates divergence between the microcharacteristics (such as micropolarity, microviscosity, etc.) of red blood cell membranes for two patients from some average values. We should note that, in the course of the bathochromic shift, no substantial variation in the shape of the fluorescence spectra is discovered. Figure 4 illustrates this, showing the fluorescence spectra of 1-AN in erythrocyte ghosts obtained using excitation frequencies near the maximum and at the red edge of the absorption spectrum.

As mentioned above, the inhomogeneous spectral broadening allows us to excite selectively, at the red edge of the absorption spectrum, the probe molecules located in different sites. In this situation it is possible to study the distribution of local dielectric constants (or, better, dielectric interactions) in model membranes using excitation by different wavelengths. To prove this we performed a spectral study, presented in the next section.

DIELECTRIC INTERACTIONS IN ERYTHROCYTE GHOSTS

The determination of ground- and excited-state dipole moments of large polar molecules from solvent shift measurements was developed mainly between 1955 and 1965 (for review see Ref. 18). Almost all cited papers describe the solvent–solute interaction by the interaction of the total (permanent plus induced) dipole moment of the solute with the local reactive field, which is described by Onsager's model.

Later, in biophysics, equations which describe the position of electronic spectra, Stokes shift of fluorescence, etc., dependent on the electrical properties of solvent and solute molecules, were applied to study the local dielectric properties in biological systems. However, very little work has been done on local dielectric properties of membranes, despite their potential significance. We have studied dielectric interactions in human erythrocyte ghosts using a 1-AN probe in combination with red-edge excitation spectroscopy. The values of the local dielectric constant ε of erythrocyte ghosts were calculated from the following equation, which is a modified variant of Eq. 243 from Ref. 18, neglecting all polarizability terms:

$$hc\tilde{\nu}_{fl} = \text{const} + \frac{1}{2\pi\varepsilon_0 a_0^3}\left[\frac{n^2-1}{2(2n^2+1)}|\Delta^e\boldsymbol{\mu}|^2 - \frac{\varepsilon-1}{2\varepsilon+1}(\Delta^e\boldsymbol{\mu},\boldsymbol{\mu}_e)\right] \quad (15)$$

where $\tilde{\nu}_{fl}$ is the average of the half-height points of the normalized quantum fluorescence spectrum $\Phi_s(\tilde{\nu})/\tilde{\nu}^3$; μ_e is the dipole moment in the equilibrated excited state, $\Delta^e\mu$ is the change in the dipole moment vector after transition from the equilibrated excited state to the Franck–Condon ground state, n is the refractive index, a_0 is the probe cavity radius, h is the Plank constant, and c is the light velocity. As follows from data above, the dipole moment of 1-AN in the equilibrium ground state is roughly equal to zero. Because 1-AN is a rigid molecule, we may assume that the dipole moment in the Franck–Condon ground state also has a small value. Hence the term $\Delta^e\mu$ in good approximation may be chosen equal to $\Delta^a\mu = 16.0 \times 10^{-30}$ Cm as for 1-AN in cyclohexane.

Estimation of the dielectric constant by Eq. (15) is most convenient in our case, because only the position of the fluorescence spectrum of probe molecules located in different sites may be measured with sufficient accuracy. Equation (15), which relates the fluorescence spectrum maximum with dipole moments, is valid for one type of emitting species in one well-defined solvent environment with a low enough viscosity. Because in our case different sites contribute to the measured fluorescence spectrum, the local dielectric constant ε determined from Eq. (15) is an average value. We have measured the time-resolved fluorescence spectra and fluorescence anisotropy kinetics and have found that the intermolecular relaxation time for 1-AN in erythrocyte ghosts lies mainly in the subnanosecond region, i.e., is lower in relation to the mean fluorescence lifetime ($\langle\tau_0\rangle$ = 7 ns). Thus the viscosity of the membrane is low enough and Eq. (15) is a good approximation for 1-AN erythrocyte ghosts.

The probe cavity radius or the spherical Onsager parameter a_0 is essential for accurate determination of the dielectric constant. In order to estimate this value with a high accuracy we measured the fluorescence quantum spectrum for 1-AN in a set of aprotic solvents with different refractive indexes and dielectric constants. From fitting by Eq. (15) the experimentally measured function $\Phi_s(\tilde{\nu})$ divided by $\tilde{\nu}^3$, it follows that a_0 = 2.78 Å for the 1-AN probe. This value is smaller than a_0 determined from the molecule volume.[31,33] This is not surprising because the 1-AN molecule has an essentially nonspherical shape and it is not so easy to estimate the

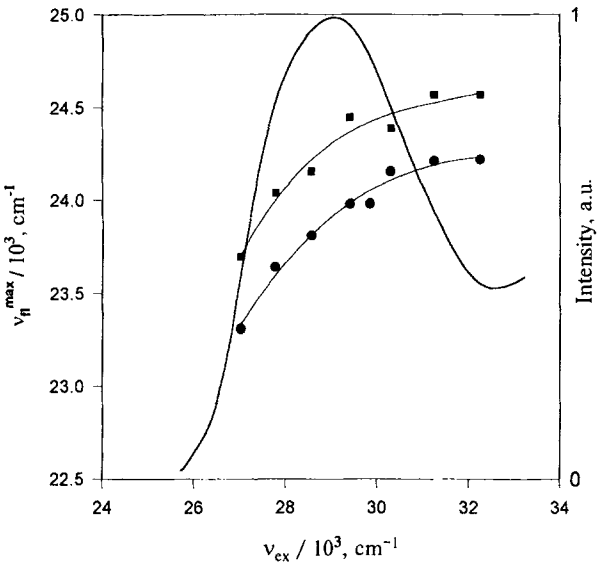

Fig. 3. The maximum of the fluorescence spectra of 1-AN in human erythrocyte ghosts as the function of the excitation frequencies for two probes of blood. The solid line represents the excitation spectrum.

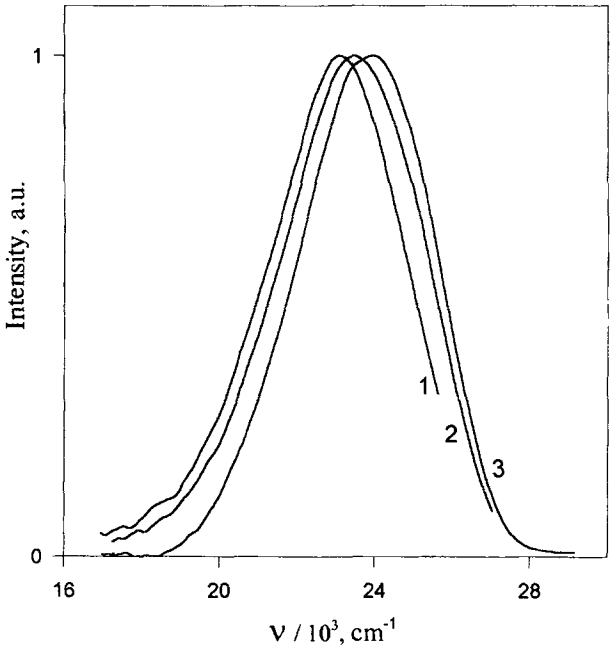

Fig. 4. The steady-state fluorescence spectra of 1-AN in human erythrocyte ghosts at different excitation frequencies: (1) ν_{ex} = 27,000 cm^{-1}; (2) ν_{ex} = 28,600 cm^{-1}; (3) ν_{ex} = 31,300 cm^{-1}.

spherical Onsager parameter from geometrical sizes of molecule.

In Table V the values of the dielectric constant ε of human erythrocyte ghosts are presented as calculated by Eq. (15). The calculations were performed with the assumption $\Delta^e\boldsymbol{\mu} \| \boldsymbol{\mu}_e$ that is sufficiently valid for many molecules. The value of the refractive index n = 1.425 was taken as for lipid vesicles.[44] It is shown in Table V that the dielectric constant increases from ε = 6.7 ± 0.8 at ν_{ex} = 32,300 cm^{-1} to ε = 17.6 ± 3.5 at ν_{ex} = 27,000 cm^{-1}. This effect is caused by selective excitation, at the long-wavelength edge of the absorption spectrum, of the "red" sites located in more polar regions of erythrocyte ghosts.

The results obtained in this section prove that there exists a probe molecule distribution over sites with different micropolarities.

Table V. Dielectric Constant (ε) Estimated for Different Excitation Frequencies ν_{ex} of 1-AN in Human Erythrocyte Ghosts[a]

ν_{ex} (cm^{-1})	ε
32,300 ± 100	6.7 ± 0.8
31,300 ± 100	6.9 ± 1.0
30,300 ± 100	7.3 ± 1.8
29,400 ± 100	8.1 ± 1.4
28,600 ± 100	8.5 ± 0.9
27,800 ± 100	10.8 ± 1.4
27,000 ± 100	17.6 ± 3.5

[a] The value of ε for each excitation frequency is an average value obtained from five independent experiments with different probes of blood.

CONCLUSIONS

Our results show that the charge distribution in 1-AN differs substantially from that in 1,8-ANS. The dipole moment of 1-AN in the equilibrated ground state $\boldsymbol{\mu}_g$ has a very small value, roughly equal to zero. The vectors $\mathbf{m}_a$ and $\Delta^a\boldsymbol{\mu}$ for 1-AN are parallel, and upon optical excitation, the dipole moment increases by 16.0 × 10^{-30} Cm in cyclohexane and 18.8 × 10^{-30} Cm in dioxane.

In the case of 1,8-ANS in dioxane the transition dipole moment $\mathbf{m}_a$ is perpendicular to the dipole moment in the equilibrium ground state $\boldsymbol{\mu}_g$ and the angles between the vectors $\mathbf{m}_a$, $\boldsymbol{\mu}_g$, $\Delta^a\boldsymbol{\mu}$, and $\boldsymbol{\mu}_e^{FC}$ are in the range 18–108°. The dipole moments $\boldsymbol{\mu}_g$, $\Delta^a\boldsymbol{\mu}$, and $\boldsymbol{\mu}_e^{FC}$ have values within the range (19.4–23.3) × 10^{-30} Cm. The spectral dependence of electrooptical coefficients for 1,8-ANS indicates that the first absorption band is a su-

perposition of several (at least two) electronic transitions.

We found that the electronic spectra of 1-AN in erythrocyte ghosts are inhomogeneously broadened. This broadening manifests itself as a red shift of the steady-state fluorescence spectrum on excitation at the long-wavelength edge of the absorption spectrum. The dielectric constant of human erythrocyte ghosts varies between 6.7 ± 0.8 to 17.6 ± 3.5, depending on the excitation frequency and, consequently, on the location of 1-AN probe molecules.

ACKNOWLEDGMENTS

Financial support by a Deutsche Forschungsgemeinschaft (DFG) fellowship (to N.A.N.) is gratefully acknowledged. We thank Dr. N. Detzer and Mrs. G. Bormann for purification of the fluorescence probes and solvents and Mr. E. Petrov for assistance with time-resolved measurements. This work was supported partly by ISTC Grant B-78, Fund of Fundamental Research of Belarus, Grant F-94/135, and Fonds der Chemischen Industrie, Germany.

REFERENCES

1. L. Brand and J. R. Gohlike (1972) *Annu. Rev. Biochem.* **41**, 843–868.
2. G. K. Radda (1971) *Biochem. J.* **122**, 385–396.
3. H. Azzi (1975) *Q. Rev. Biophys.* **8**, 237.
4. D. Chapman (1975) *Q. Rev. Biophys.* **8**, 185.
5. J. R. Lakowicz (1983) *Principles of Fluorescent Spectroscopy*, Plenum Press, New York.
6. A. P. Demchenko (1986) *Ultraviolet Spectroscopy of Proteins*, Springer-Verlag, Berlin.
7. G. E. Dobretsov (1989) *Fluorescent Probes for Studying Cells, Membranes and Proteins*, Nauka, Moscow.
8. C. J. Seliskar and L. Brand (1971) *J. Am. Chem. Soc.* **93** (21), 5405–5420.
9. G. Weber and D. J. R. Laurence (1954) *Biochem. J.* **56**, xxxi.
10. H. Träuble and P. Overath (1973) *Biochim. Biophys. Acta* **307**, 491–512.
11. H. Träuble and H. Eibl (1974) *Proc. Natl. Acad. Sci. USA* **71**, 214–219.
12. F. Bellemare and M. Fragata (1980) *J. Coll. Interf. Sci.* **77**, 243–252.
13. M. Fragata and F. Bellemare (1985) *J. Coll. Interf. Sci.* **107**, 553–559.
14. Y. Kimura and A. Ikegami (1985) *J. Membr. Biol.* **85**, 225–231.
15. N. A. Nemkovich, A. N. Rubinov, and M. G. Savvidi (1992) *Inst. Phys. Conf. Ser.* **126**, 639–642.
16. N. A. Nemkovich and A. N. Rubinov (1995) *J. Fluoresc.* **5**, 285–294.
17. E. Liptay (1974) in E. C. Lim (Ed.), *Excited States, Vol. 1*, Academic Press, New York, pp. 129–229.
18. W. Baumann (1989) in B. W. Rossiter and J. F. Hamitton (Eds.), *Physical Methods of Chemistry, Vol. 3b*, Wiley, pp. 45–131.
19. W. Rettig and W. Baumann (1992) in J. F. Ralek (Ed.), *Progress in Photochemistry and Photophysics, Vol. VI*, CRC Press, Boca Raton, pp. 79–134.
20. N. A. Nemkovich, W. Baumann, H. Reis, and N. Detzer (1995) *J. Photochem. Photobiol. A Chem.* **89**, 127–133.
21. W. Baumann and H. Bishof (1982) *J. Mol. Struct.* **84**, 181–193.
22. W. Baumann and H. Bishof (1985) *J. Mol. Struct.* **129**, 125–136.
23. N. A. Nemkovich, A. S. Kozlovsky, A. N. Rubinov, and Yu. V. Zvinevich (1995) *Proc. SPIE* **2388**, 347–355.
24. B. Valuer and J. Moirez (1973) *J. Chim. Phys. Physicochim. Biol.* **70**, 500–506.
25. G. H. Golub and C. Reinsch (1970) *Num. Math.* **14**, 403–420.
26. G. Striker (1982) in M. Bouchy (Ed.), *Deconvolution and Reconvolution of Analytical Signals*, University Press, Nancy, pp. 329–357.
27. J. A. Nelder and R. Mead (1965) *Comp. J.* **7**, 308–313.
28. R. Fletcher (1970) *Comp. J.* **13**, 317–322.
29. J. A. Riddick, W. B. Bunger, and T. K. Sakano (1986) *Organic Solvents*, John Wiley & Sons.
30. J. T. Dodge, C. Mitchell, and D. J. Hanahan (1963) *Arch. Biochem. Biophys.* **100**, 119–130.
31. M. Kumbar and V. T. Maddaiah (1977) *Biochim. Biophys. Acta* **497**, 707–718.
32. J. C. Smith and R. W. Woody (1976) *J. Phys. Chem.* **80**, 1094–1100.
33. V. A. Kawski and B. Pasztor (1966) *Acta Phys. Polonica* **XXIX**, 187–193.
34. E. M. Kosower and H. Dodiuk (1974) *Chem. Phys. Lett.* **26**, 545–548.
35. E. M. Kosower, H. Dodiuk, K. Tanizawa, M. Ottolenghi, and N. Orbach (1975) *J. Am. Chem. Soc.* **97**, 2167–2178.
36. E. M. Kosower (1982) *Acc. Chem. Res.* **15**, 259–266.
37. E. M. Kosower and D. Huppert (1986) *Annu. Rev. Phys. Chem.* **47**, 127.
38. Y.-H. Li, L.-M. Chan, L. Tyer, R. T. Moody, C. M. Himel, and D. M. Hercules (1975) *J. Am. Chem. Soc.* **97**, 3118–3126.
39. T. W. Ebbesen and C. A. Ghiron (1989) *J. Phys. Chem.* **93**, 7139–7143.
40. N. A. Nemkovich, V. I. Tomin, and A. N. Rubinov (1991) in J. R. Lakowicz (Ed.), *Topics in Fluorescence Spectroscopy, Vol. 2. Principles*, Plenum Press, New York, pp. 367–428.
41. D. M. Gakamsky, A. P. Demchenko, N. A. Nemkovich, A. N. Rubinov, V. I. Tomin, and N. V. Shcherbatska (1992) *Biophys. Chem.* **42**, 49–61.
42. N. A. Nemkovich (1992) *Proc. SPIE*, **1922**, 209–218.
43. N. A. Nemkovich, A. S. Kozlovsky, and A. N. Rubinov (1995) *Proc. SPIE* **2388**, 389–399.
44. D. Toptygin and L. Brand (1993) *Biophys. Chem.* **48**, 205–220.